Appl Nanosci (2016) 6:965–972
DOI 10.1007/s13204-015-0513-8

ORIGINAL ARTICLE

Synthesis, characterization and photocatalytic applications of Zn-doped TiO_2 nanoparticles by sol–gel method

Dinkar V. Aware[1] · **Shridhar S. Jadhav**[2]

Received: 9 June 2015 / Accepted: 25 November 2015 / Published online: 14 December 2015

Abstract Mesoporous, nanocrystalline, Zinc-doped TiO_2 nanoparticles were synthesized by surfactant-assisted sol–gel method. The X-ray diffraction (XRD), scanning electron microscopy (SEM), transmission electron microscopy (TEM), Brunauer–Emmett–Teller (BET), and UV–VIS spectrometer techniques were used to characterize the synthesized products. XRD results confirm the formation of the anatase phase for the TiO_2 nanoparticles, with crystallite sizes in the range of 12.6–18.1 nm. The small crystallite size and doping with Zinc ion inhibit phase transformation and promote the growth of the TiO_2 anatase phase. The SEM and TEM micrographs revealed the spherical-like morphology with average diameter of about 12–18 nm which is in agreement with XRD results. The optical study shows that doping ions lead to an increase in the absorption edge wavelength and a decrease in the band gap energy of titania. Photocatalytic activity of the synthesized nanomaterials was successfully tested for photodegradation of methyl red as model pollutant under UV light. The photocatalytic activity results confirm that the doped nanoparticles show higher activity than undoped titania. The small grain size, high crystallinity, high specific surface area and decrease in the band gap energy of doped titania may be responsible for the high photocatalytic activity.

Keywords Sol–gel · XRD · SEM-EDX · TEM · BET · UV-DRS · Photodegradation of methyl red

✉ Dinkar V. Aware
awaredinkar@gmail.com

Shridhar S. Jadhav
ssjadhav1957@gmail.com

[1] Department of Chemistry, Arts, Commerce and Science College Sonai, Affiliated to S. P. Pune University, Tal. Newasa, Ahmednagar, India

[2] P.G. Department of Chemistry, New Arts, Commerce and Science College Ahmednagar, Affiliated to S.P. Pune University, Ahmednagar, India

Introduction

Over the past decades, semiconducting photocatalytic materials like ZnO, TiO_2 are widely applied for degradation and complete mineralization of toxic organic compounds in water, soil, and air (Zeng et al. 2008; Qian et al. 2009). Titania (TiO_2) based catalyst is widely applied for decomposition of toxic organic chemicals both in the aqueous and gas phase due to its unique properties like nontoxicity, chemical stability, high photocatalytic activity and low cost. However, its widespread application is still limited because of the high band gap energy of photocatalytically active titania (3.2 eV for anatase TiO_2). It requires UV irradiation; solar light contains only a small fraction of (about 4–5 %) UV light, therefore, it is necessary to develop a photocatalyst that could be activated under visible light irradiation in order to use sunlight as a chief energy source.

The photocatalytic activity of titania can be improved by decrease in grain size, increasing surface area, sensitization using dye molecules and doping with metals and non-metals (Zhang et al. 2010; Fu et al. 1996). Doping with transition metal ions like Fe^{2+}, Mn^{2+}, Cu^{2+}, Zn^{2+}, etc. (Kubacka et al. 2009) is the one of the most powerful way to improve the photocatalytic activity of titania. Of all the transition metal ions, Zn^{2+} causes more effective doping with titania since ionic radii of Zn^{2+} (0.74 Å) and Ti^{4+} (0.75 Å) are similar to each other (Rauf et al. 2011).

Hence Zn^{2+} ion can easily substitute Ti^{4+} ion in TiO_2 lattice without destroying the crystal structure, thereby stabilizing the anatase phase. Recently, Zn-doped TiO_2 powder was synthesized by various preparative methods like sol-hydrothermal (Yang et al. 2010; Zhu et al. 2012); sol–gel and solid phase reaction (Liu 2005); homogeneous hydrolysis (Österlund et al. 2009); controlled hydrolysis of titanium(IV) butoxide (Mahata et al. 2011); electrospinning (Khajavi and Abbasipour 2012); assembly process based on Ligand exchange reaction (Xu et al. 2005) micro emulsion (Sanchez-Dominguez et al. 2015) and sol–gel method (Seabra et al. 2011; Chauhan et al. 2012).

Sol–gel method is one of the most versatile technique generally adapted for the synthesis of metal-doped nanocrystalline titania; it has some advantages over other conventional methods like good homogeneity, control grain size, particle morphology and porosity. Surfactant-assisted sol–gel method was widely used to synthesize mesoporous materials (Jentys et al. 1996; Beck et al. 1992; Wang et al. 1999; Tanev et al. 1997).With successfully synthesized MCM-like mesoporous material (Liu et al. 2004; Yang et al. 2015), it is believed that nanoparticles of zinc-doped titania could be possible to synthesize using similar surfactant-assisted sol–gel method.

In this article, a very simple, ecofriendly straightforward, catalyst free, surfactant template assisted, single step sol–gel process in alcohol–water mixed solution was reported. A potential technique for nanocrystalline mesoporous undoped and zinc-doped TiO_2 nanoparticle synthesis. The photocatalytic activities of as synthesized catalyst were thoroughly studied in relating to its photocatalytic activity of methyl red photodegradation. The satisfactorily high photocatalytic efficiency was attained by doped samples as compared to undoped titania.

Experimental

Chemicals

For the synthesis of pure TiO_2 and zinc-doped TiO_2 nanoparticles, the materials used were titanium (IV) butoxide [$M = 340.76$, Ti $(OC_4H_9)_4$], zinc nitrate [$M = 297$, Zn $(NO_3)_2{\cdot}6H_2O$], obtained from Sigma-Aldrich, cetyltrimethyl ammonium bromide [$M = 364.46$, C_{19} $H_{42}BrN$], Isopropyl Alcohol [$M = 60$, $(CH_3)_2CHOH$], were obtain from SD Fine Chemicals and ethyl alcohol [$M = 46$, C_2H_5OH] from local distillery. The titanium (IV) butoxide and Zn $(NO_3)_2{\cdot}6H_2O$ were used as the precursors for the TiO_2 and Zn components, respectively, and deionized water was used as a solvent.

Synthesis

Synthesis of TiO_2 nanoparticles

Pure TiO_2 nanoparticles were synthesized by sol–gel method. A solution containing 160 ml of ethanol and 20 ml of iso-propanol was mixed slowly with 20 ml (50 mmol) of Titanium (IV) butoxide under sonication. The resultant mixture was slowly added to 100 ml of deionized water containing 2 g of cetyltrimethyl ammonium bromide (CTAB) to form a white precipitate. The system was kept under constant stirring at 80 °C for 4 h. The excess water was removed by evaporation on the water bath with continuous stirring. The resultant precursor was then dried at 110 °C for 12 h and then finally calcined at 500 °C for 4 h in high temperature muffle furnace.

Synthesis of series of Zn-doped TiO_2

The Zn-doped TiO_2 nanoparticles was synthesized using the same method as that of TiO_2, except that the water used for the synthesis (100 ml) contained the required amount of zinc nitrate (1, 3 and 5 mol%).

Evaluation of photocatalytic activity of the samples

In this study, the photocatalytic activity was tested using methyl red (MR) solution as a model pollutant under UV light radiation. The photocatalytic degradation was carried out with 100 ml aqueous methyl red solution (100 ppm) containing 50 mg of catalyst nanoparticles. This mixture was stirred in dark for 30 min to reach adsorption equilibrium. Then, the mixture was placed inside the photoreactor in which the vessel was 3.5–4 cm away from the UV lamp. The quartz vessel and the light source were placed inside a black box to prevent UV leakage. The experiments were performed at room temperature and a pH of about 6.3. Small portions of the mixture were taken at periodic intervals during the irradiation, and after centrifugation, they were analyzed with the UV–Vis spectrophotometer. The % mineralization of dye was determined by COD measurement following the closed reflux volumetric method.

Characterization

The synthesized materials were characterized by various sophisticated Techniques. X-ray diffraction (XRD) patterns were carried out by using Philips X-ray diffractometer with diffraction angle 2θ in between 20° and 80° using Cu-Kα radiation of wavelength 1·542 Å. Surface morphology and elemental analysis of the samples were carried out using

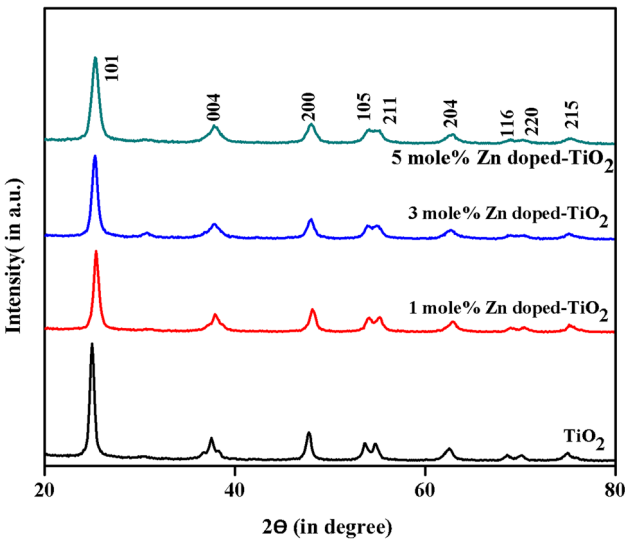

Fig. 1 XRD Pattern of pure TiO_2 and zinc doped TiO_2 nanoparticles calcined at 500 °C

scanning electron microscopy with electron dispersion spectroscopy (SEM–EDS) characterization conducted using a JEOL-JED 2300 (LA) instrument. The microscopic nanostructure and particle size was determined using a CM-200 PHILIPS transmission electron microscope (TEM) at 200 kV ($L = 600$, $\lambda = 0.0025$ nm). The surface area of the samples was determined from nitrogen adsorption–desorption isotherms at liquid nitrogen temperature using a Quantachrome ASiQwin1994–2013 instrument with out gas 15 min at 150 °C. The BET method was used for surface area calculation (Brunauer et al. 1938), the pore size distribution (pore diameter and pore volume of the samples) was determined by the BJH method (Barrett et al. 1951). The light absorption by sample was carried out using Varian Carry 5000 (UV–VIS-DRS) spectroscopy in the range 800–200 nm.

Results and discussion

X-Ray diffraction of doped and pure TiO_2

Figure 1 shows XRD patterns of the pure TiO_2 and Zn-doped TiO_2 with different dopant concentrations calcined at 500 °C. All the samples exhibit anatase phase with no evidence of rutile phase and zinc ions. The existence of zinc ion is confirmed by EDX (see Fig. 3).

Also, the sharp, intense peak at $2\theta = 25.281°$ corresponds to anatase (101) phase, representing that the synthesized nanomaterials were well crystallized. All the diffraction peaks obtained from XRD agreed with the reported JCPDS card no. 21-1272 for anatase. The crystallite sizes were estimated by the Scherrer's equation, using the most intense reflection ($2\theta = 25.281°$).When the mol% of the zinc ion doping in TiO_2 was increased, the crystallite size decreased. The particle sizes in the samples were in the range of 12.6–18.1 nm when calcined at 500 °C.

Scanning electron microscopy (SEM) analysis

SEM analysis was carried out for two representative samples calcined at 500 °C, named as TiO_2 and 5 mol% Zn-doped TiO_2, the results are shown in Fig. 2. As it follows from the SEM micrographs, synthesized nanoparticles are spherical in shape. A slight agglomeration was seen in both samples.

Energy dispersive X-ray spectroscopy (EDS) analysis

Energy dispersive X-ray spectroscopy (EDS) analysis was also carried out for 5 mol% Zn-doped TiO_2 (Fig. 3) and the result shows that the Ti and Zn atomic % in the obtained

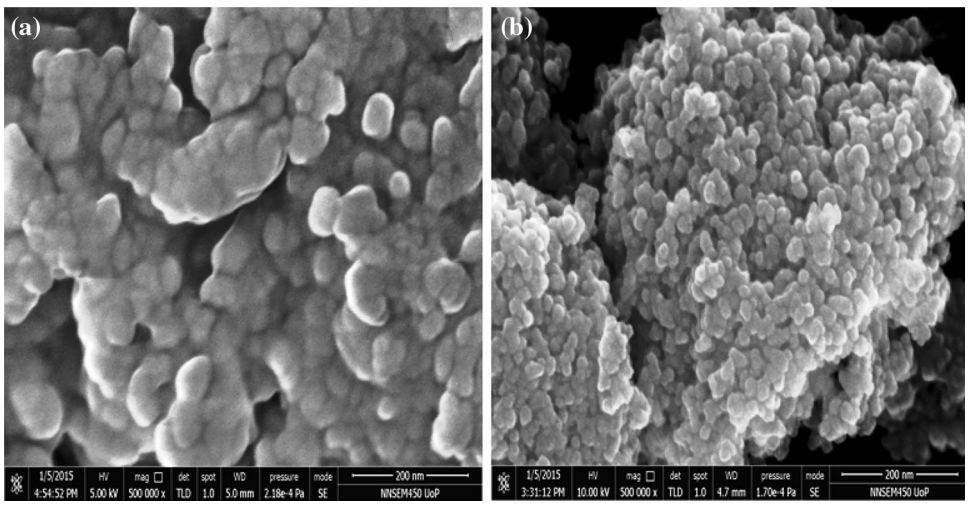

Fig. 2 SEM micrographs of the synthesized nanoparticles: **a** Pure TiO_2 and **b** 5 mol Zn-doped TiO_2 calcined at 500 °C with CTAB at different magnification

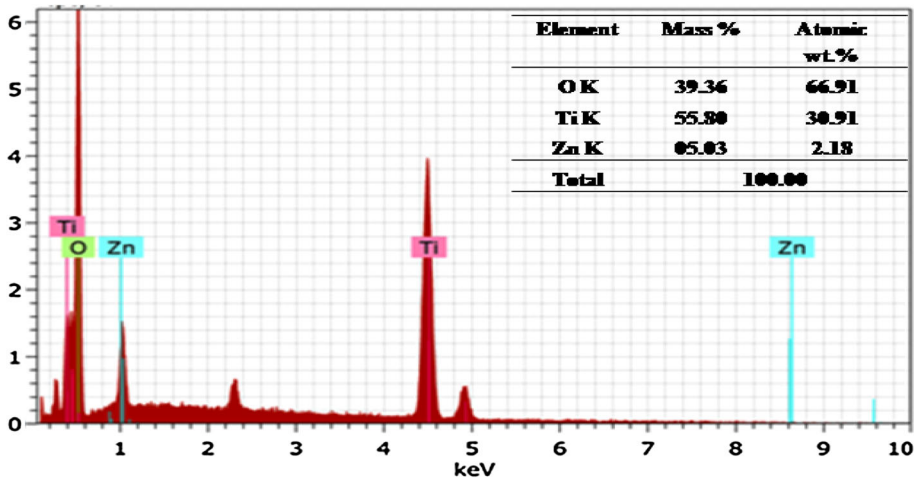

Fig. 3 Energy dispersive X-ray analysis of 5 mol% Zn-doped TiO_2 nanoparticles calcined at 500 °C with CTAB

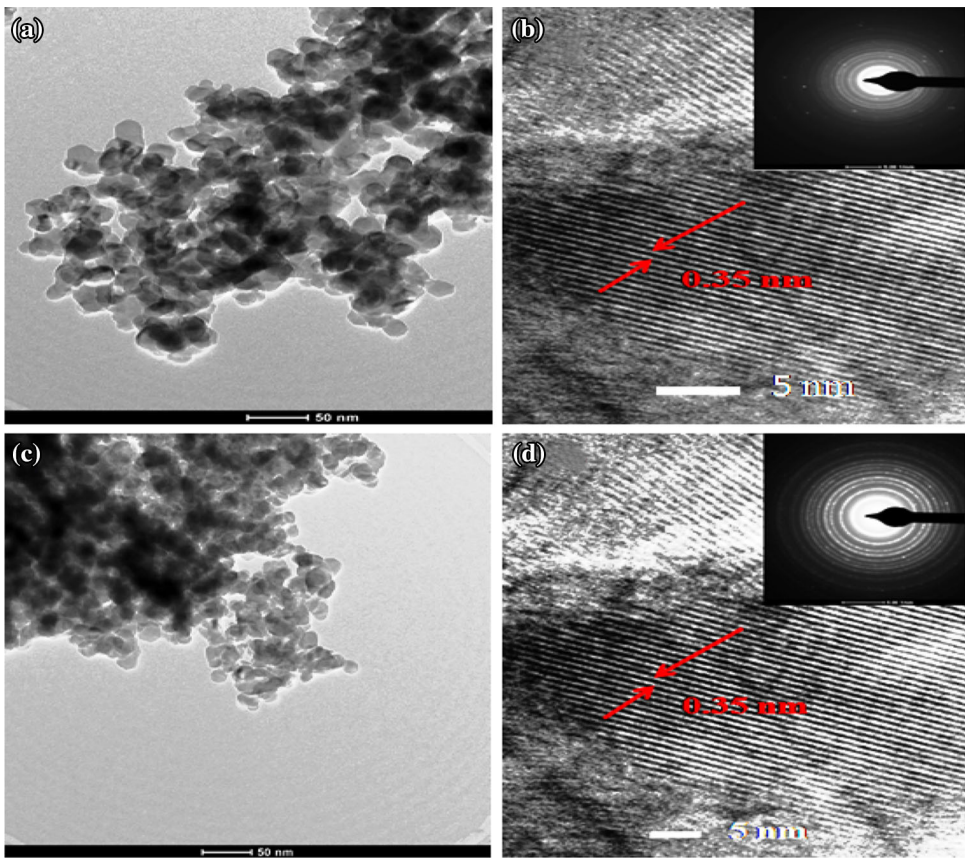

Fig. 4 TEM micrographs of synthesized nanoparticles: **a**, **b** Pure TiO_2; **c**, **d** 5 mol% Zn-doped TiO_2. The *inset* of **b** and **d** shows the corresponding SAED pattern, calcined at 500 °C with CTAB at different magnification

materials is in very good agreement with the nominal (expected) composition.

Transmission electron microscopy (TEM) analysis

By HRTEM it was possible to carry out an assessment of particle size, morphology and crystallinity. Figure 4 shows results for pure TiO_2 and 5 mol% Zn-doped TiO_2. In Fig. 4a and b, it can be observed that nanoparticles of TiO_2 have a spherical shape and a size around 14–18 nm. Figure 4b shows that the particles are crystalline, as evidenced by the lattice fringes observed. Selected Area electron diffraction (SAED) analysis of the nanocrystals in Fig. 4b is shown as inset; the calculated d-spacing was 0.350536 nm which is in agreement with (*hkl*) (internuclear distance of anatase TiO_2 phase (JCPDS 21-1272).

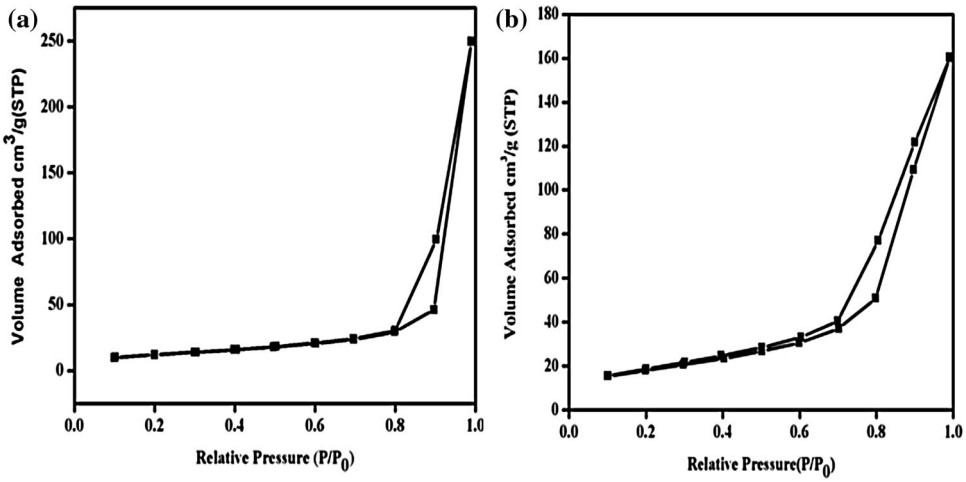

Fig. 5 Nitrogen adsorption–desorption of **a** TiO_2, **b** 5 mol% Zn-doped TiO_2

5 mol% Zn-doped TiO_2 nanoparticles were also spherical in shape, and the particle size was in the order of 12–14 nm, as shown in Fig. 4c; lattice fringes were also observed for this sample, as shown in Fig. 4d (calculated d-spacing was 0.351802 nm, which is in agreement with (hkl) (101) of anatase TiO_2 phase, JCPDS 21-1272).

BET surface area

Figure 5 shows the N_2 adsorption–desorption isotherm of two representative synthesized samples i.e. Pure TiO_2 and 5 mol% Zn-doped TiO_2. According to IUPAC the entire synthesized sample shows a type IV isotherm with hysteresis loop indicates existence of mesopores which provides highest photocatalytic activity towards methyl red. The multipoint BET specific surface area for both studied catalyst was found to be 43.376 and 63.667 m^2/g, respectively, these values are higher than non-porous TiO_2 materials (2–30 m^2/g). Our findings clearly indicates that Zn-doped TiO_2 have a larger surface area and a greater N_2 adsorption capacity than pure TiO_2, which is due to the increase in the pore size. Table 1 shows the physical parameters of nitrogen isotherms, such as BET surface area (S_{BET}), BJH average pore diameter (d_p) and the pore volume (V_p).

UV–visible diffusion reflectance spectroscopy (UV-DRS)

The band gap energies (E_{bg}) of the synthesized nanomaterials were calculated by using UV–visible diffusion reflectance spectroscopy (DRS). To determine band gap energy of the synthesized materials, the diffusion reflectance spectra were recorded and cut off wave length at which absorption sharp edge rises were determined by drawing a tangent on this curves (Fig. 6). The band gap energies were calculated using cut-off wavelength and are

Table 1 Band gap energies of the synthesized photocatalyst

Photocatalyst	TiO_2	1 mol% Zn-TiO_2	3 mol% Zn-TiO_2	5 mol% Zn-TiO_2
Band gap e(in eV)	2.96	2.92	2.91	2.83

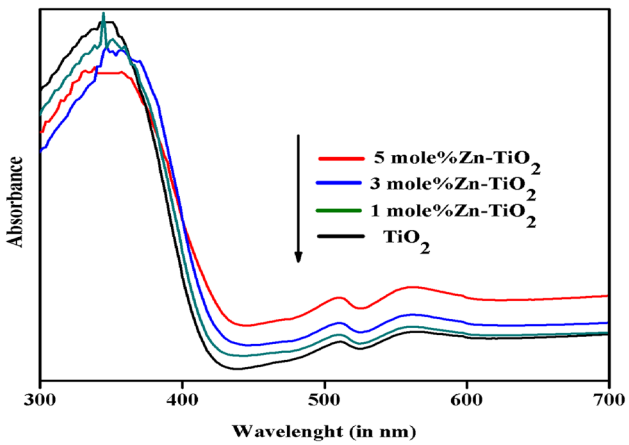

Fig. 6 UV-DRS image of pure and Zn-doped TiO_2 nanoparticles

represented in the following table. The band gap energy is calculated using the following equation (Bhatkhande et al. 2002):

$$E_{bg} = \frac{1240}{\lambda}$$

where λ is the wavelength in nanometer and E_{bg} is the band gap energy.

From the results of band gap energy data (Table 2), we can conclude that pure TiO_2 had weak visible light response than Zn-doped TiO_2, i.e. due doping ability of light absorption of TiO_2 is slightly enhanced.

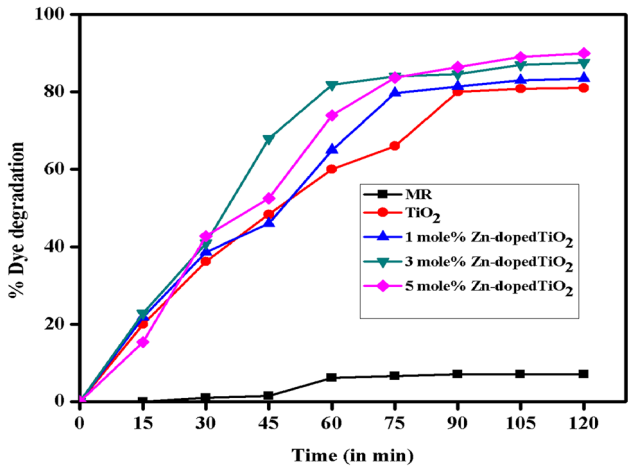

Fig. 7 Temporal evolution of MR removal during photocatalytic experiments under UV light irradiation

Photocatalytic activity result

Photocatalytic activities of the synthesized nanomaterials were tested using methyl red as a model pollutant. Methyl red is from synthetic azo dye and according to International Agency for Research on Cancer (IARC) is probably carcinogenic to human beings. Methyl red is a major water pollutant and its degradation to safe levels is not an easy task due to its resistance to chemical and biological degradation.

The photocatalytic activity study of synthesized nanomaterials was carried out under UV light irradiation and the results of photocatalytic performance are shown in the Figs. 7 and 8. From Fig. 7 we can conclude that removal of dye reaches an approximately constant value after 75 min of photocatalytic treatment for all the tested photocatalyst

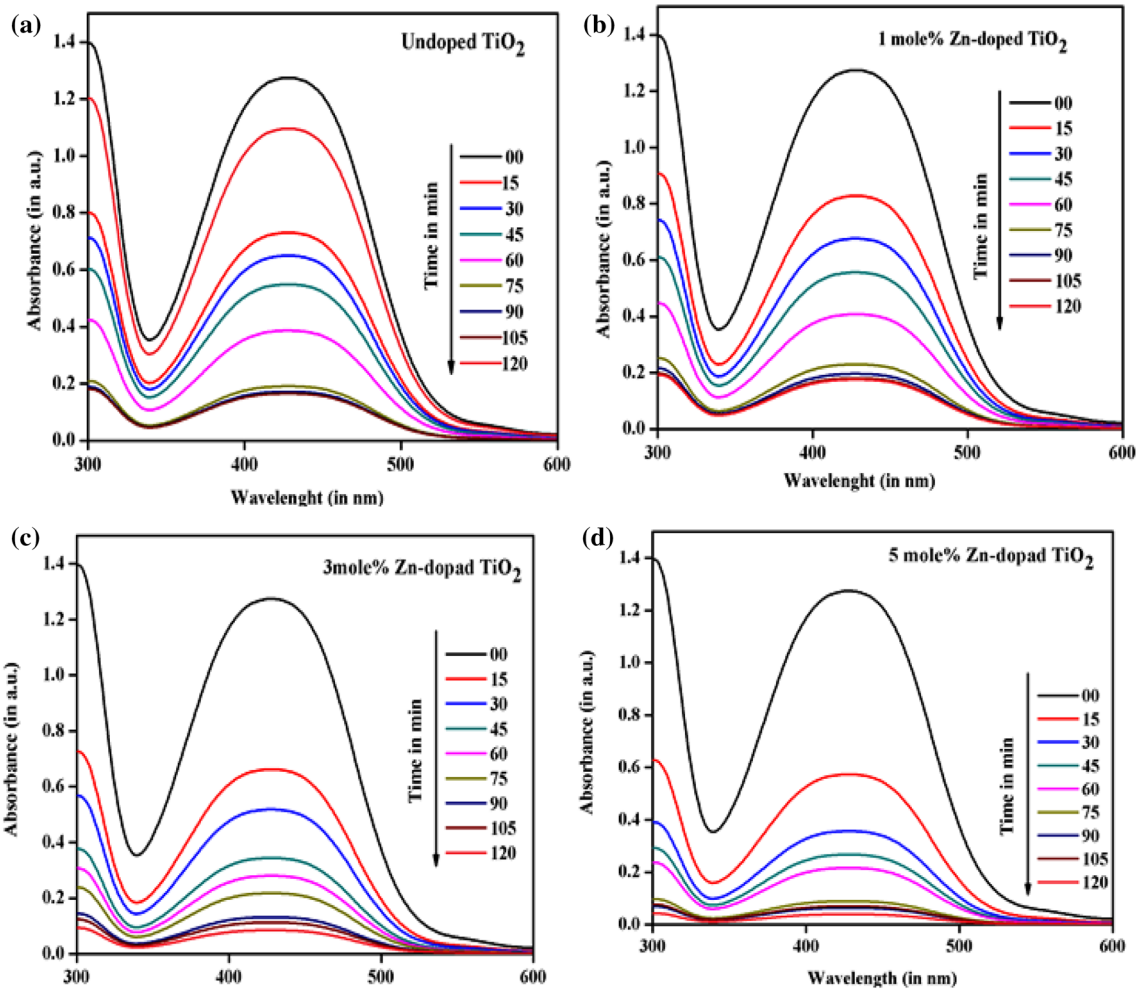

Fig. 8 Photodegradation graphs of methyl red with **a** Pure TiO_2, **b** 1 mol% Zn-doped TiO_2, **c** 3 mol% Zn-doped TiO_2, and **d** 5 mol% Zn-doped TiO_2

Table 2 Degradation and mineralization results obtained after 2 h for TiO_2 and Zn- doped TiO_2

Photocatalyst	%Degradation (UV–Vis) time: 2 h	%Mineralization time: 2 h
TiO_2	86.2	82
1 mol% Zn-dopedTiO_2	87.05	84
3 mol% Zn-doped TiO_2	93.33	89
5 mol% Zn-doped TiO_2	96.99	93

and also methyl red removal achieves values between 86 and 96.99 % after 120 min of irradiation time, presenting the 5 mol% Zn-doped TiO_2 the almost photodegradation under UV light (93 and 96.99 % removal of methyl red after 75 and 120 min of irradiation time, respectively) among the studied photocatalyst. Table 2 shows % methyl red photocatalytic removal after 2 h under both UV light irradiation.

It is important to note that the photocatalytic reaction does not take place at all in the absence of a photocatalyst. Additionally, if the mixture of methyl red and the synthesized catalyst are kept in the dark for more than 24 h, no significant degradation of dye takes place. When the reaction mixture containing methyl red and catalyst is kept under visible light, photodegradation takes place, but the reaction takes a very long time compared to the degradation that occurs in the presence of UV light. The higher photocatalytic activity of doped TiO_2 under UV irradiation is attributed due to its smaller grain size high surface area narrower band gap energy.

Conclusion

Herein, we report very simple route for synthesis of mesoporous nanocrystalline Zn-doped TiO_2 nanoparticles via sol–gel technique using CTAB as surface directing agent. The XRD pattern of all synthesized samples calcined at 500 °C confirms the formation anatase phase with very good crystallinity. From the XRD, SEM-EDX, TEM, BET, and UV–Vis results, it was confirmed that the doping of Zinc in TiO_2 decreases the grain size and shifts the absorption to higher wavelengths. The results of photocatalytic study confirm the highest photodegradation of methyl red under UV irradiation for 5 mol% of Zn-doped TiO_2 compared to other synthesized catalyst.

Acknowledgments The authors are grateful to the Principal, Arts Commerce and Science College Sonai, as well as thanking to the Principal, New Arts, Commerce and Science College Ahmednagar for providing the all required facilities to carry out the work.

References

Barrett EP, Joyner LG, Halenda PP (1951) The determination of pore volume and area distributions in porous substances. I. Computations from nitrogen isotherms. J Am Chem Soc 73:373–380. doi:10.1021/ja01145a126

Beck JS, Vartuli JC, Roth WJ, Leonowicz ME, Kresge CT, Schmitt KD, Chu CT-W, Olson DH, Sheppard EW, McCullen SB, Higgins JB, Schlenkert JL (1992) A new family of mesoporous molecular sieves prepared with liquid crystal templates. J Am Chem Soc 10834–10843. doi:10.1021/ja00053a020

Bhatkhande DS, Pangarkar VG, Beenackers AACM (2002) Photocatalytic degradation for environmental applications—a review. J Chem Technol Biotechnol 77:15. doi:10.1002/jctb.532

Brunauer S, Emmett PH, Teller E (1938) Gases in multimolecular layers. J Am Chem Soc 60:309–319. doi:10.1021/ja01269a023

Chauhan R, Kumar A, Chaudhary R (2012) Structural and optical characterization of Zn doped TiO2 nanoparticles prepared by sol–gel method. J Sol-gel Sci 585–591. doi:10.1007/s10971-011-2664-8

Fu X, Clark LA, Yang Q, Anderson MA (1996) Enhanced Photocatalytic Performance of Titania-Based Binary Metal Oxides: TiO 2 /SiO2 and TiO2 /ZrO2. Environ Sci Technol 30:647–653. doi:10.1021/es950391v

Jentys A, Pham NH, Vinek H, Englisch M, Lercher JA (1996) Synthesis and characterization of mesoporic materials containing highly dispersed cobalt. Microporous Mater 6:13–17. doi:10.1016/0927-6513(95)00079-8

Khajavi R, Abbasipour M (2012) Electrospinning as a versatile method for fabricating coreshell, hollow and porous nanofibers. Sci Iran 19:2029–2034. doi:10.1016/j.scient.2012.10.037

Kubacka A, Colón G, Fernández-García M (2009) Cationic (V, Mo, Nb, W) doping of TiO2-anatase: a real alternative for visible light-driven photocatalysts. Catal Today 143:286–292. doi:10.1016/j.cattod.2008.09.028

Liu G (2005) The preparation of Zn 2+ -doped TiO_2 nanoparticles by sol–gel and solid phase reaction methods respectively and their photocatalytic activities 59:1367–1371. doi:10.1016/j.chemosphere.2004.11.072

Liu Z, Hu Z, Liang J, Li S, Yang Y (2004) Size-controlled synthesis and growth mechanism of monodisperse tellurium nanorods by a surfactant-assisted method 214–218

Mahata S, Mahato SS, Nandi MM, Mondal B (2011) Synthesis of TiO_2 nanoparticles by hydrolysis and peptization of titanium isopropoxide solution. AIP Conf Proc 1461:225–228. doi:10.1063/1.4736892

Österlund L, Štengl V, Mattsson A, Bakardjieva S, Andersson PO, Opluštil F (2009) Effect of sample preparation and humidity on the photodegradation rate of CEES on pure and Zn doped anatase TiO_2 nanoparticles prepared by homogeneous hydrolysis. Appl Catal B Environ 88:194–203. doi:10.1016/j.apcatb.2008.09.029

Qian J, Liu P, Xiao Y, Jiang Y, Cao Y, Ai X, Yang H (2009) TiO_2-coated multilayered SnO2 hollow microspheres for dye-sensitized solar cells. Adv Mater 21:3663–3667. doi:10.1002/adma.200900525

Rauf MA, Meetani MA, Hisaindee S (2011) An overview on the photocatalytic degradation of azo dyes in the presence of TiO_2 doped with selective transition metals. Desalination 276:13–27. doi:10.1016/j.desal.2011.03.071

Sanchez-Dominguez M, Morales-Mendoza G, Rodriguez-Vargas MJ, Ibarra-Malo CC, Rodriguez-Rodriguez AA, Vela-Gonzalez AV, Perez-Garcia SA, Gomez R (2015) Synthesis of Zn-doped TiO_2 nanoparticles by the novel oil-in-water (O/W) microemulsion method and their use for the photocatalytic degradation of phenol. J Environ Chem Eng. doi:10.1016/j.jece.2015.03.010

Seabra MP, Salvado IMM, Labrincha JA (2011) Pure and (zinc or iron) doped titania powders prepared by sol-gel and used as photocatalyst. Ceram Int 37:3317–3322. doi:10.1016/j.ceramint.2011.04.127

Tanev PT, Liang Y, Pinnavaia TJ (1997) Assembly of mesoporous lamelar silicas with hierarchical particle architectures. J Am Chem Soc 119:8616–8624. doi:10.1021/ja970228v

Wang Y, Cheng H, Hao Y, Ma J, Li W, Cai S (1999) Photoelectrochemical properties of metal-ion-doped TiO_2 nanocrystalline electrodes. Thin Solid Films 349:120–125. doi:10.1016/S0040-6090(99)00239-4

Xu J, Lu M, Guo X, Li H (2005) Zinc ions surface-doped titanium dioxide nanotubes and its photocatalysis activity for degradation of methyl orange in water. J Mol Catal A Chem 226:123–127. doi:10.1016/j.molcata.2004.09.051

Yang L, Zhang Y, Ruan W, Zhao B, Xu W, Lombardi JR (2010) Improved surface-enhanced Raman scattering properties of TiO_2 nanoparticles by Zn dopant. J Raman Spectrosc 41:721–726. doi:10.1002/jrs.2511

Yang Y-J, Kelkar AV, Zhu X, Bai G, Ng HT, Corti DS, Franses EI (2015) Effect of sodium dodecylsulfate monomers and micelles on the stability of aqueous dispersions of titanium dioxide pigment nanoparticles against agglomeration and sedimentation. J Colloid Interface Sci 450:434–445. doi:10.1016/j.jcis.2015.02.051

Zeng H, Cai W, Liu P, Xu X, Zhou H, Klingshirn C, Kalt H (2008) ZnO-based hollow nanoparticles by selective etching: elimination and reconstruction of metal—semiconductor interface, improvement of blue emission and photocatalysis. ACS Nano 2:1661–1670. doi:10.1021/nn800353q

Zhang J, Wu Y, Xing M, Leghari SAK, Sajjad S (2010) Development of modified N doped TiO_2 photocatalyst with metals, nonmetals and metal oxides. Energy Environ Sci 3:715. doi:10.1039/b927575d

Zhu F, Zhang P, Wu X, Fu L, Zhang J, Xu D (2012) The origin of higher open-circuit voltage in Zn-doped TiO_2 nanoparticle-based dye-sensitized solar cells. ChemPhysChem 13:3731–3737. doi:10.1002/cphc.201200362